Inorganic Chemistry
Article

Inorg. Chem. **2009**, *48*, 5313–5319 **5313**
DOI: 10.1021/ic9002884

Synthesis and Structural and Physical Properties of New Semiconducting Quaternary Tellurides: $Ba_4Ag_{3.95}Ge_2Te_9$ and $Ba_4Cu_{3.71}Ge_2Te_9$

Yanjie Cui, Abdeljalil Assoud, and Holger Kleinke*

Department of Chemistry, University of Waterloo, Waterloo, ON, Canada N2L 3G1

Received February 11, 2009

Two quaternary tellurides, $Ba_4Ag_{3.95}Ge_2Te_9$ and $Ba_4Cu_{3.71}Ge_2Te_9$, were prepared in evacuated silica tubes at 750 °C. Both tellurides crystallize in space group *Pbam*, with lattice parameters of a = 8.6835(3) Å, b = 13.6421(4) Å, c = 10.2612(3) Å, and V = 1215.55(7) Å^3 (Z = 2) for $Ba_4Ag_{3.95}Ge_2Te_9$ and a = 8.6464(2) Å, b = 13.5305(4) Å, c = 10.0810(3) Å, and V = 1179.38(6) Å^3 (Z = 2) for $Ba_4Cu_{3.71}Ge_2Te_9$. These structures are comprised of planar Ag_4/Cu_4 clusters and dimeric Ge_2Te_6 units, which are interconnected through Te atoms into a three-dimensional structure. Several split sites in the case of $Ba_4Cu_{3.71}Ge_2Te_9$ are reflected in additional, different clusters, including a linear Cu_3 unit. The covalent Ag−Te/Ge−Te network surrounds a one-dimensional linear channel running along the *c* direction, encompassing the Ba atoms. Electronic structure calculations and transport property measurements show that these two compounds are *p*-type semiconductors with calculated band gaps of 0.24 eV for the Ag compound and 1.0 eV for the Cu compound.

Introduction

The thermoelectric properties[1−3] of several binary, ternary, and quaternary copper and silver tellurides have been examined for several years, including $Cu_{2-\delta}Te$,[4] α- and β-Ag_2Te,[5] $BaCu_2Te_2$,[6] $A_2BaCu_8Te_{10}$ (A = K, Rb, Cs),[7] Ag_8GeTe_6,[8] AgTlTe,[9] $AgSbTe_2$,[10] $Ag_{3-\delta}Sb_{1+\delta}Te_4$,[11] $(AgBiTe_2)_{1-\delta}(Ag_2Te)_\delta$,[12] $(AgSbTe_2)_{1-\delta}(GeTe)_\delta$ (TAGS),[13,14] and $AgPb_mSbTe_{2+m}$.[15] In recent years, we have been exploring the properties of a number of ternary Cu/Ag tellurides, that is, $Ba_3Cu_{14}Te_{12}$,[16] $Ba_7M_2Te_{14}$,[17] and BaM_2Te_2[18] (M = Cu, Ag, or Au) with various bonding M−M interactions and band gaps ranging from 0.5 to 1.0 eV. Here, we report on our first quaternary barium silver/copper germanium tellurides that are the first members of that system. Moreover, very few Ba−Cu/Ag−Ge sulfides and selenides are known, namely, the sulfides $BaCu_2GeS_4$,[19] $BaAg_2GeS_4$,[20] and $BaCu_6Ge_2S_8$[21] as well as the selenides $BaCu_2GeSe_4$ and $BaAg_2GeSe_4$.[22] All of the sulfides and selenides comprise the elements in the most common oxidation states, namely, Ba^{2+}, Cu^+, Ag^+, Ge^{IV}, S^{2-}, and Se^{2-}. Their structures are generally composed of MQ_4 and GeQ_4 (Q = S, Se) tetrahedra, while one Cu atom of $BaCu_6Ge_2S_8$ is only bonded to three S atoms. The tellurides introduced here exhibit different oxidation states and structural features and are black in contrast to the mostly red sulfides and selenides.

*To whom correspondence should be addressed. E-mail: kleinke@uwaterloo.ca.

(1) Tritt, T. M. *Science* **1999**, *283*, 804–805.
(2) DiSalvo, F. J. *Science* **1999**, *285*, 703–706.
(3) Rowe, D. M. *CRC Handbook of Thermoelectrics*; CRC Press: Boca Raton, FL, **1995**.
(4) Sridhar, K.; Chattopadhyay, K. *J. Alloys Compd.* **1998**, *264*, 293–298.
(5) Fujikane, M.; Kurosaki, K.; Muta, H.; Yamanaka, S. *J. Alloys Compd.* **2005**, *393*, 299–301.
(6) Wang, Y. C.; DiSalvo, F. J. *J. Solid State Chem.* **2001**, *156*, 44–50.
(7) Patschke, R.; Zhang, X.; Singh, D.; Schindler, J.; Kannewurf, C. R.; Lowhorn, N.; Tritt, T.; Nolas, G. S.; Kanatzidis, M. G. *Chem. Mater.* **2001**, *13*, 613–621.
(8) Fujikane, M.; Kurosaki, K.; Muta, H.; Yamanaka, S. *J. Alloys Compd.* **2005**, *396*, 280–282.
(9) Kurosaki, K.; Uneda, H.; Muta, H.; Yamanaka, S. *J. Alloys Compd.* **2005**, *395*, 304–306.
(10) Hagiwara, E.; Matsushita, H.; Katsui, A. *J. Adv. Science* **2000**, *12*, 40–41.
(11) Matsushita, H.; Hagiwara, E.; Katsui, A. *J. Mater. Sci.* **2004**, *39*, 6299–6301.
(12) Sakakibara, T.; Imoto, T.; Takigawa, Y.; Kurosawa, K. *J. Adv. Science* **2001**, *12*, 392–396.
(13) Skrabek, E. A.; Trimmer, D. S. Properties of the general TAGS system. In *CRC Handbook of Thermoelectrics*; Rowe, D. M., Ed.; CRC Press: Boca Raton, FL, **1995**; pp 267−275.
(14) Shelimova, L. E.; Konstantinov, P. P.; Karpinsky, O. G.; Avilov, E. S.; Kretova, M. A.; Fleurial, J. P. *Int. Conf. Thermoelectr.* **1999**, *18*, 536–540.
(15) Hsu, K. F.; Loo, S.; Guo, F.; Chen, W.; Dyck, J. S.; Uher, C.; Hogan, T.; Polychroniadis, E. K.; Kanatzidis, M. G. *Science* **2004**, *303*, 818–821.
(16) Assoud, A.; Thomas, S.; Sutherland, B.; Zhang, H.; Tritt, T. M.; Kleinke, H. *Chem. Mater.* **2006**, *18*, 3866–3872.
(17) Cui, Y.; Assoud, A.; Xu, J.; Kleinke, H. *Inorg. Chem.* **2007**, *46*, 1215–1221.
(18) Assoud, A.; Cui, Y.; Thomas, S.; Sutherland, B.; Kleinke, H. *J. Solid State Chem.* **2008**, *181*, 2024–2030.
(19) Teske, C. L. *Z. Naturforsch., B: Chem. Sci.* **1979**, *34*, 386–389.
(20) Teske, C. L. *Z. Naturforsch., B: Chem. Sci.* **1979**, *34*, 544–547.
(21) Tampier, M.; Johrendt, D. *Z. Naturforsch., B: Chem. Sci.* **1998**, *53*, 1483–1488.
(22) Tampier, M.; Johrendt, D. *Z. Anorg. Allg. Chem.* **2001**, *627*, 312–320.

Published on Web 05/08/2009

Experimental Section

Syntheses and Analyses. These two tellurides $Ba_4Ag_{3.95}Ge_2Te_9$ and $Ba_4Cu_{3.71}Ge_2Te_9$ were prepared by heating the elements in evacuated silica tubes up to 750 °C. All elements were obtained with purities of at least 99%: barium granules, 99%, Aldrich; silver powder −22 mesh, 99.9995%, Alfa Aesar; copper powder −625 mesh, 99.9%, Alfa Aesar; germanium powder −100 mesh, 99.99%, Aldrich; and tellurium powder, −200 mesh, 99.9%, Alfa Aesar. These were stored in an argon-filled glovebox. In the glovebox, the starting materials, Ba, Ag, Ge, and Te, were loaded in the molar ratio of 4:4:2:9 into a fused silica tube, which was then sealed under a high vacuum of approximately 10^{-2} mbar. The reaction mixture was heated to 750 °C within 48 h in a resistance furnace, kept at that temperature for 2 h, and then cooled to 200 °C at a rate of 3 °C per hour, followed by switching off the furnace. An X-ray powder diffractogram (using the Inel diffractometer with Cu $K\alpha_1$ radiation) obtained from the ground sample showed that no known materials were present, indicating the formation of at least one new material. After successful structure solution, the melting point of $Ba_4Ag_4Ge_2Te_9$ was determined to be 728 °C using the Netzsch Luxx DSC.[23]

The copper analog was prepared using the same temperature profile, but a subsequent single-crystal structure study revealed a significant deviation from the 4:4:2:9 ratio of the elements, namely, a Cu deficiency, with the refined formula being $Ba_4Cu_{3.71}Ge_2Te_9$.

No heteroelements, such as silicon that might have come from the silica tube, were found during the subsequent energy dispersive X-ray analysis (EDAX) on selected crystals of both $Ba_4Ag_4Ge_2Te_9$ and $Ba_4Cu_{3.71}Ge_2Te_9$, using a LEO 1530 electron microscope with an additional EDAX device, the EDAX Pegasus 1200.

Crystal Structure Determinations. Single-crystal data collections were carried out on a Smart Apex CCD (BRUKER) equipped with an area detector utilizing graphite-monochromatic Mo Kα. Data were collected by scans of 0.3° in ω at different φ angles, for an overall of 2×606 frames with exposure times of 30 s each. The data were corrected for Lorentz and polarization effects. Absorption corrections were based on fitting a function to the empirical transmission surface, as sampled by multiple measurements of numerous symmetry equivalent reflections.[24] Structure solution and refinements were performed with the SHELXTL package.[25]

The structure solution via direct methods led to the identification of eight sites for the Ag case, occupied by one Ba, two Ag, one Ge, and four Te atoms. The refinements of this model resulted in R1 = 0.0166 and wR2 = 0.0349 (observed data) with every site fully occupied. Since the displacement factor of Ag1 was 8% higher than that of Ag2, the occupancy of Ag1 was refined, revealing a small though significant deficiency of 2.7(2)%. This occurred with significantly[26] improved residual values, R1 = 0.0154 and wR2 = 0.0327. To further investigate the Ag1 deficiency, a second crystal was selected from another sample starting from 4:4:2:9 Ba/Ag/Ge/Te. The refinement results are highly consistent, with a Ag1 deficiency of 2.3(2)% and residual values of R1 = 0.0217 and wR2 = 0.0298. Finally, the atomic positions were standardized with the TIDY program within the PLATON package.[27]

Table 1. Crystallographic Data of $Ba_4Ag_{3.95}Ge_2Te_9$ (left) and $Ba_4Cu_{3.71}Ge_2Te_9$ (right)

refined formula	$Ba_4Ag_{3.946(4)}Ge_2Te_9$	$Ba_4Cu_{3.71(2)}Ge_2Te_9$
fw [g/mol]	2268.49	2078.93
T of measurement [K]	296(2)	296(2)
wavelength [Å]	0.71073	0.71073
cryst syst	orthorhombic	orthorhombic
space group	*Pbam*	*Pbam*
a [Å]	8.6835(3)	8.6464(2)
b [Å]	13.6421(4)	13.5305(4)
c [Å]	10.2612(3)	10.0810(3)
V [Å^3]	1215.55(7)	1179.38(6)
Z	2	2
ρ_{calcd} [g/cm^3]	6.198	5.854
R1 and wR2 (all data)[a]	0.0160, 0.0329	0.0236, 0.0475
R1 and wR2 ($I > 2\sigma(I)$)[a]	0.0154, 0.0327	0.0218, 0.0466

[a] $R1 = \sum||F_o| - |F_c||/\sum|F_o|$; $wR2 = [\sum[w(F_o^2 - F_c^2)^2]/\sum[w(F_o^2)^2]]^{1/2}$.

To check for the phase range, another crystal was analyzed from a new Ag-deficient sample of nominal formula "$Ba_4Ag_{3.1}Ge_2Te_9$", resulting in a slightly higher Ag deficiency, as expressed in the refined formula $Ba_4Ag_{3.902(6)}Ge_2Te_9$. Hence, a small phase range may be formulated for $Ba_4Ag_{4-x}Ge_2Te_9$ with $0.05 < x < 0.10$.

The structure solution of the Cu compound initially yielded an isostructural model. For ease of comparison, the Ag solution with all positions fully occupied was used in the following refinement steps. This resulted in rather high R values: R1 = 0.0701 and wR2 = 0.1639 (observed reflections). Due to the conspicuously high displacement factors, U_{eq}, of Cu1, 0.54(3) Å^2; Cu2, 0.0494(11) Å^2; Te3, 0.0303(4) Å^2; and Te4, 0.0448(9) Å^2 combined with large anisotropies, these atoms were refined as split sites (e.g., Cu1 and Cu1A) one by one. More uniform U_{eq} values and gradually improving R values were obtained, and the occupancies of the Cu1 atoms were refined as well, giving R1 = 0.0299 and wR2 = 0.0706. Thereby, Te4 moved from the 2a site to 4g, that is, from point group $2/m$ to m. Because the resulting Fourier map contained an additional electron density peak close to Cu1A, another split site, Cu1B, was introduced. This led to a featureless electron density map and significantly lower residual values of R1 = 0.0218 and wR2 = 0.0466. These improvements were all significant at the 0.005 confidence level of the Hamilton test.[26] The occupancies of Cu1, Cu1A, and Cu1B were refined to 45%, 22%, and 25%, respectively, the occupancies of Cu2 and Cu2A to 89% and 12%, and those of Te3 and Te3A to 87% and 13%, respectively. The refined formula is thus $Ba_4Cu_{3.71(2)}Ge_2Te_9$.

To find the lower limit of the Cu occupancy, a second crystal was analyzed from a more Cu-deficient starting composition, namely, 4:3.1:2:9 Ba/Cu/Ge/Te. The refinement yielded the same split sites and formula within standard deviation, namely, $Ba_4Cu_{3.70(1)}Ge_2Te_9$ with R1 = 0.0294 and wR2 = 0.0564, so that the phase range was concluded to be minimal. Detailed crystal structure information is listed in Tables 1 and 2.

Electronic Structure Calculations. We utilized the self-consistent tight-binding *first principles* linear muffin-tin orbitals (LMTO) method, with the atomic spheres approximation[28,29] for the electronic structures calculation. In the LMTO approach, the density functional theory is employed utilizing the local density approximation for the exchange and correlation energies.[30] The following wave functions were used: for Ba, 6s and 5d, 6p, and 4f via the downfolding technique; for Ag, 5s,

(23) Lee, C.-S.; Kleinke, K. M.; Kleinke, H. *Solid State Sci.* **2005**, *7*, 1049–1054.
(24) *SAINT,* version 4; Siemens Analytical X-ray Instruments Inc.: Madison, WI, **1995**.
(25) Sheldrick, G. M. *SHELXTL,* version 5.12; Siemens Analytical X-Ray Systems: Madison, WI, **1995**.
(26) Hamilton, W. C. *Acta Crystallogr.* **1965**, *18*, 502–510.
(27) Spek, A. L. *J. Appl. Crystallogr.* **2003**, *36*, 7–13.
(28) Andersen, O. K. *Phys. Rev. B* **1975**, *12*, 3060–3083.
(29) Skriver, H. L. *The LMTO Method;* Springer: Berlin, Germany, **1984**.
(30) Hedin, L.; Lundqvist, B. I. *J. Phys. C* **1971**, *4*, 2064–2083.
(31) Lambrecht, W. R. L.; Andersen, O. K. *Phys. Rev. B* **1986**, *34*, 2439–2449.

Table 2. Atomic Coordinates and Equivalent Displacement Parameters of $Ba_4Ag_{3.95}Ge_2Te_9$ and $Ba_4Cu_{3.71}Ge_2Te_9$

atom	site	*x*	*y*	*z*	U_{eq}/Å$^{2\,a}$	occ.
			$Ba_4Ag_{3.95}Ge_2Te_9$			
Ba	8i	0.37968(2)	0.32391(1)	0.23993(2)	0.01521(6)	1
Te1	8i	0.25031(2)	0.06300(2)	0.29184(2)	0.01381(6)	1
Te2	4 h	0.09896(3)	0.28005(2)	0.5	0.01462(7)	1
Te3	4 g	0.08035(3)	0.31419(2)	0	0.01401(7)	1
Te4	2a	0	0	0	0.01510(9)	1
Ag1	4 g	0.26150(5)	0.12478(3)	0	0.0275(2)	0.973(2)
Ag2	4f	0	0.5	0.14071(4)	0.0268(1)	1
Ge	4 h	0.41797(5)	0.07233(3)	0.5	0.01200(9)	1
			$Ba_4Cu_{3.71}Ge_2Te_9$			
Ba	8i	0.38575(3)	0.32114(2)	0.24098(3)	0.01849(7)	1
Te1	8i	0.26121(3)	0.06176(2)	0.28142(3)	0.01903(8)	1
Te2	4 h	0.10616(4)	0.28046(3)	0.5	0.01569(9)	1
Te3	4 g	0.07657(7)	0.32458(5)	0	0.0221(2)	0.870(2)
Te3A	4 g	0.1149(5)	0.2800(4)	0	0.0221(2)	0.130
Te4	4 g	0.0274(1)	0.0032(2)	0	0.0187(3)	0.5
Cu1	4 g	0.2345(3)	0.4825(2)	0	0.0427(9)	0.447(5)
Cu1A	4 g	0.2607(9)	0.1423(7)	0	0.057(2)	0.219(3)
Cu1B	4 g	0.2874(8)	0.1010(6)	0	0.058(2)	0.247(4)
Cu2	4f	0	0.5	0.1371(1)	0.0424(4)	0.886(4)
Cu2A	2c	0	0.5	0	0.0424(4)	0.114
Ge	4 h	0.41879(8)	0.07237(5)	0.5	0.0164(1)	1

[a] U_{eq} is defined as one-third of the trace of the orthogonalized U_{ij} tensor.

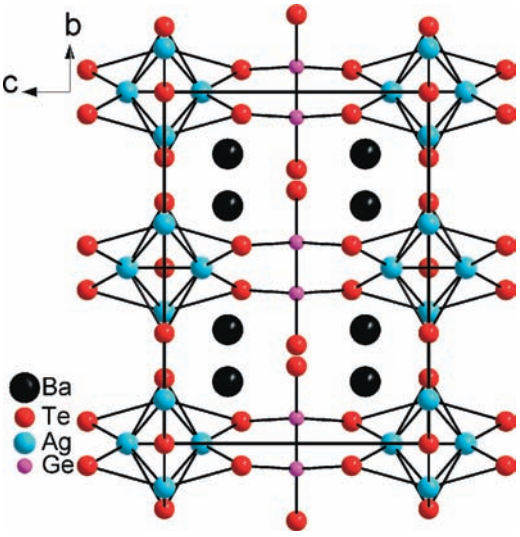

Figure 1. Crystal structure of $Ba_4Ag_{3.95}Ge_2Te_9$.

5p, 4d, and 4f (downfolded); for Cu, 4s, 4p, and 3d; for Ge, 4s, 4p, and 4d (downfolded); and for Te, 5s, 5p, 5d, and 4f (the latter two downfolded). The integrations in *k* space were performed on a grid of 2080 independent *k* points of the first Brillouin zone via an improved tetrahedron method.[32] To model the electron-precise formula $Ba_4Ag_4Ge_2Te_9$, we treated all Ag sites as fully occupied. In the Cu case, we calculated three models: two thereof with the Cu1, Cu2, and Te3 sites fully occupied, while in the first model Te4 was located on the 4g site (formally 50%, necessitating symmetry reduction to $Pb2_1m$) and in the second Te4 was placed on the high-symmetry 2a site, like in the Ag case. These two models of the formula $Ba_4Cu_4Ge_2Te_9$ have almost identical band structures. The third model was based on the Cu2A and Cu1A sites, having a Cu-deficient formula of $Ba_4Cu_3Ge_2Te_9$ and a linear Cu_3 unit instead of the Cu_4 cluster of $Ba_4Cu_4Ge_2Te_9$.

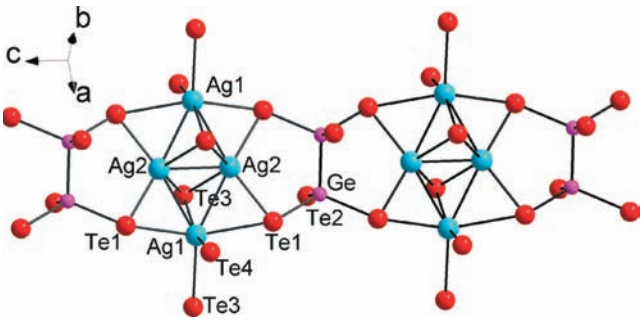

Figure 2. Fragment of the covalent framework of $Ba_4Ag_{3.95}Ge_2Te_9$ comprising Ag_4 clusters and Ge_2Te_6 units.

Transport Measurements. Cold pressed bars of dimensions 5 × 1 × 1 [in mm] for samples $Ba_4Ag_{3.95}Ge_2Te_9$ and $Ba_4Cu_{3.7}Ge_2Te_9$ were used for physical transport measurements, since no single crystals of sufficient dimensions were available. Silver paint (Ted Pella) was used to create the electric contacts. The Seebeck coefficient, *S*, was determined with a commercial thermopower measurement apparatus (MMR Technologies) under a dynamic vacuum in the temperature range from 300 to 550 K. Constantan was used as an internal standard to determine the temperature difference. The specific electrical conductivity, σ, was determined using a four-point-method: a homemade device was used to determine the voltage drops ΔV over distances (*L*) of approximately 1 mm at currents of 1 mA under a dynamic vacuum between 320 and 190 K or 180 K. The achieved densities were between 84% and 85% of the theoretical maxima as determined via the single-crystal structure studies. The resistances (*R*) were calculated from the voltage drops using Ohm's law, that is, $R = \Delta V/I$, with I = current. We calculated σ(T) after measuring the lengths between the contacts, *L*, according to $\sigma = L/(AR)$, with the area A = 1 mm × 1 mm.

Results and Discussion

Crystal Structures. These two new quaternary tellurides, $Ba_4Ag_{3.95}Ge_2Te_9$ and $Ba_4Cu_{3.71}Ge_2Te_9$, crystallize in their own new three-dimensional structure type, as shown in Figure 1 for $Ba_4Ag_{3.95}Ge_2Te_9$, wherein the Ba−Te bonds are omitted for clarity. The Ba atoms are surrounded by eight Te atoms in a bicapped trigonal prism, with distances in the range of 3.49−3.77 Å for $Ba_4Ag_{3.95}Ge_2Te_9$ and 3.42−3.69 Å for $Ba_4Cu_{3.71}Ge_2Te_9$. These distances are comparable to the Ba−Te bonds of the nine-fold coordinated Ba atoms in $BaSbTe_3$ (3.41−3.89 Å),[33] Ba_2SnTe_5 (3.44−3.84 Å),[34] and $Ba_3Cu_{14}Te_{12}$ (3.47−3.84 Å).[16]

The structure motifs include $BaTe_8$ bicapped trigonal prisms, $AgTe_4$ tetrahedra, $AgTe_5$ square pyramids, and dimeric Ge_2Te_6 units. The Ag1 atoms are surrounded by five Te atoms to form a square pyramid with Ag−Te distances ranging from 2.84 to 3.11 Å (Figure 2). The corresponding Cu atom splits into three sites, Cu1, Cu1A, and Cu1B, with occupancies of 44.7%, 21.9%, and 24.7%, respectively. The short distances (0.60−2.16 Å) between these three atoms necessitate that they are never occupied at the same location within a given

(32) Blöchl, P. E.; Jepsen, O.; Andersen, O. K. *Phys. Rev. B* **1994**, *49*, 16223–16233.

(33) Volk, K.; Cordier, G.; Cook, R.; Schäfer, H. *Z. Naturforsch., B: Chem. Sci.* **1980**, *35*, 136–140.

(34) Assoud, A.; Derakhshan, S.; Soheilnia, N.; Kleinke, H. *Chem. Mater.* **2004**, *16*, 4193–4198.

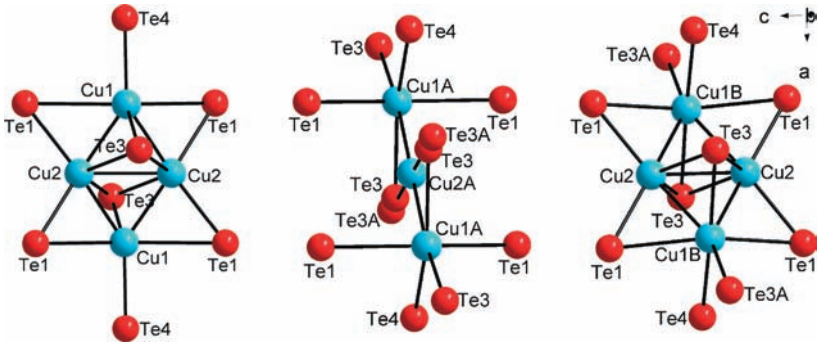

Figure 3. Split site variants of the Cu clusters with surrounding Te atoms of $Ba_4Cu_{3.71}Ge_2Te_9$.

crystal; this concurs well with the combined occupancies being below 100% (overall occupancy 91.3%). Such a scenario is common in copper chalcogenides, for example, in $LnCu_{0.3-0.4}Te_2$,[35] $Gd_3Cu_2Te_7$,[36] $Cu_{2-\delta}Se$,[37] $CuSm_3Se_6$,[38] and $Cu_4Bi_4Se_9$.[39]

The tetrahedrally coordinated Ag2/Cu2 atoms connect with two Te1 and two Te3 atoms at distances of 2.80 and 3.00 Å for Ag2 and 2.66 and 2.82 Å for Cu2. Two $Ag1Te_5$ square pyramids and two $Ag2Te_4$ tetrahedra are interconnected to each other by edge-sharing, forming a planar Ag_4 cluster with Ag−Ag distances of 2.89 Å (Ag2−Ag2) and 3.04 Å (Ag1−Ag2). The Ag_4Te_{10} units are connected through dimeric Ge_2Te_6 units to a complex one-dimensional chain running along the *c* axis.

It is noted that the Ag1−Ag2 bond is longer than Ag2−Ag2, while the Cu1−Cu2 bond of $Ba_4Cu_{3.71}Ge_2Te_9$ (2.47 Å) is shorter than Cu2−Cu2 (2.76 Å). Another important difference between the Cu and Ag tellurides is the long Cu1−Te3 distance >4 Å compared to the Ag1−Te3 distance of 3.03 Å. Therefore, both Cu sites, Cu1 and Cu2, are coordinated by four Te atoms (left part of Figure 3).

Furthermore, the Cu split sites cause the occurrence of other Cu clusters as well. For example, one Cu2A atom replaces two Cu2 atoms, for it is located in the center of the original Cu2 dumbbell, thus forming a linear Cu_3 unit in lieu of the Cu_4 cluster (center part of Figure 3). Thus, the Cu telluride formally forms a structure type different from that of the Ag telluride because of the additional Wyckoff position, 2c, being filled by Cu2A (and because of the Te4 site, as discussed below). Cu2A can only be surrounded by Cu1A, because the distances to Cu1 (2.04 Å) and Cu1B (2.29 Å) are both too short. Moreover, the Cu2A atom moves one Te3 atom into its Te3A split site, as the Cu2A−Te3 distance of 2.46 Å is also too short. This observation is validated by the approximately equal occupancies of 12−13% for Cu2A and Te3A. Another variant of the Cu_4 cluster is represented in the right part of Figure 3, consisting of two Cu1B and two Cu2 atoms with Cu1B−Cu2 distances of 2.68 Å. Despite the deficiencies and split sites, the Cu ions may not move through the crystals, for the clusters are surrounded by the Ge_2Te_6 units that block the path for the Cu ions. This constitutes a strong contrast to the Cu-ion-conducting selenide−telluride, $Ba_3Cu_{17-x}(Se,Te)_{11}$.[40]

A detailed examination of the interatomic distances (Table 3) also reveals different Te coordinations for the various split sites of the main atoms Cu1 and Cu2, which are both four-fold coordinated by Te atoms. Cu1A is five-fold coordinated, like Ag1, namely by two Te1 atoms at a distance of 3.04 Å, by one Te3 (2.94 Å) and either a second Te3 (2.77 Å) or Te3A (3.24 Å), and by one Te4 at either 2.76 or 3.18 Å. The case of Cu1B is similar, but two of these five distances may be quite long at 3.26 and 3.53 Å, depending on whether the Te3 or the Te3A site is filled. Cu2A stands out, because it is coordinated by two Te3 atoms at a distance of 3.14 Å, and even longer distances of 3.61 Å to four Te1 atoms complete its coordination sphere.

One Ge−Ge bond occurs in the Ge_2Te_6 unit, indicating trivalent Ge, as reported in, for example, $K_6(Ge^{III})_2Te_6$.[41] The Ge−Ge bond distances in Ag and Cu compounds are 2.43 and 2.41 Å, respectively, comparable with 2.45 and 2.46 Å in $Tl_6(Ge^{III})_2Te_6$,[42] 2.49 Å in $K_6(Ge^{III})_2Te_6$, and 2.47 Å in $Ba_2(Ge^{III})_2Te_5$.[34] The Ge−Te bonds between 2.55 and 2.59 Å for the Ag compound and 2.57 and 2.59 Å for the Cu compound are inconspicuous as well. The linear chains that are comprised of Ag_4Te_{10} and Ge_2Te_6 units are further connected by Te3 and Te4 atoms in the *a*,*b* plane to a three-dimensional network, which incorporates the eight-coordinated Ba atoms (Figure 4).

The assignment of formal charges is straightforward: since there are no Te−Te contacts < 3.57 Å, the Te atoms are viewed as Te^{2-}, and with Ge^{III} as discussed, the other elements are in their most common oxidation states, namely, Ba^{2+} and Ag^+/Cu^+, according to $(Ba^{2+})_4(Ag^+)_4(Ge^{III})_2(Te^{2-})_9$. The observation of Ag^+ and Cu^+ is typical in such chalcogenides, as is the occurrence of the Ag−Ag/Cu−Cu bonds.[16−18,40,43−45]

(35) Huang, F. Q.; Brazis, P.; Kannewurf, C. R.; Ibers, J. A. *J. Am. Chem. Soc.* **2000**, *122*, 80–86.
(36) Huang, F. Q.; Ibers, J. A. *J. Solid State Chem.* **2001**, *159*, 186–190.
(37) Machado, K. D.; de Lima, J. C.; Grandi, T. A.; Campos, C. E. M.; Maurmann, C. E.; Gasperin, A. A. M.; Souza, S. M.; Pimenta, A. F. *Acta Crystallogr., Sect. B* **2004**, *60*, 282–286.
(38) Strobel, S.; Schleid, T. *J. Solid State Chem.* **2003**, *171*, 424–428.
(39) Makovicky, E.; Søtofte, I.; Karup-Møller, S. *Z. Kristallogr.* **2002**, *217*, 597–604.
(40) Kuropatwa, B.; Cui, Y.; Assoud, A.; Kleinke, H. *Chem. Mater.* **2009**, *21*, 88–93.
(41) Dittmar, G. *Z. Anorg. Allg. Chem.* **1979**, *453*, 68–78.
(42) Assoud, A.; Kleinke, H. Unpublished work, **2006**.
(43) Assoud, A.; Cui, Y.; Thomas, S.; Sutherland, B.; Kleinke, H. *J. Solid State Chem.* **2008**, *181*, 2024–2030.
(44) Assoud, A.; Soheilnia, N.; Kleinke, H. *Chem. Mater.* **2005**, *17*, 2255–2261.
(45) Assoud, A.; Xu, J.; Kleinke, H. *Inorg. Chem.* **2007**, *46*, 9906–9911.

Table 3. Selected Interatomic Distances [Å] of $Ba_4Ag_{3.95}Ge_2Te_9$ and $Ba_4Cu_{3.71}Ge_2Te_9$[a]

		$Ba_4Ag_{3.95}Ge_2Te_9$	$Ba_4Cu_{3.71}Ge_2Te_9$
Ba−Te1		3.4923(3)	3.6354(4)
Ba−Te1		3.6086(3)	3.5186(4)
Ba−Te1		3.7703(3)	3.6936(4)
Ba−Te2		3.5720(3)	3.6008(4)
Ba−Te2		3.6636(3)	3.5129(4)
Ba−Te3/Te3A		3.5563(3)	3.6125(5)/3.421(3)
Ba−Te3		3.5826(3)	3.5371(4)/3.420(3)
Ba−Te4/Te4		3.5949(2)	3.540(2)/3.613(2)
M1−M1A/M1B			{2.16(1)}/{1.615 (8)}
M1−M2/M2A	2×	3.0449(4)	2.465(3)/{2.041(3)}
M1A−M1B			{0.604(9)}
M1A−M2/M2A			3.146(8)/2.83(1)
M1B−M2/M2A	2×		2.675(7)/{2.291(8)}
M2−M2/M2A		2.8877(8)	2.764(2)/{1.382(1)}
M1−Te1	2×	3.1125(3)	3.033(1)
M1−Te3/Te3A		2.8913(5)	2.536(3)/2.928(5)
M1−Te3/Te3A		3.0251(5)	4.231(6)/4.909(3)
M1−Te4/Te4		2.8379(4)	2.540(3)/{2.078(3)}
M1A−Te1	2×		3.039(4)
M1A−Te3/ Te3A			2.94(1)/{2.25(1)}
M1A−Te3/ Te3A			2.768(8)/3.238(9)
M1A−Te4/Te4			2.759(8)/3.175(9)
M1B−Te1	2×		2.895(2)
M1B−Te3/ Te3A			2.695(7)/3.258(9)
M1B−Te3/ Te3A			3.532(8)/2.844(9)
M1B−Te4/Te4			2.609(7)/3.07(7)
M2−Te1	2×	2.8008(3)	2.6606(7)
M2−Te3/Te3A	2×	2.9995(3)	2.8251(9)/3.429(5)
M2A−Te3/ Te3A	2×		{2.4641(7)}/3.138 (5)
M2A−Te1	4×		3.607(4)
Ge−Ge		2.4341(9)	2.410(1)
Ge−Te1	2×	2.5880(3)	2.5947(5)
Ge−Te2		2.5545(5)	2.5670(7)

[a] Unreasonable distances are in curly brackets. Two distances in one cell, separated by the slash, indicate that only one of the two will be present at a given site in the crystal.

These possibly closed-shell (d^{10}−d^{10}) interactions, depending on the exact electron count, may be understood on the basis of the hybridization of the filled d states with the nominally empty, energetically higher lying s and p orbitals.[46−48]

Electronic Structures. The electronic structure calculation was based on the models $Ba_4Ag_4Ge_2Te_9$ and $Ba_4Cu_4Ge_2Te_9$. In both cases, a forbidden gap separates the valence band from the conduction band, with the Ag telluride exhibiting the smaller gap of 0.24 eV, compared to the 1.0 eV in case of the Cu telluride. The Ag d states predominate the area below −4 eV

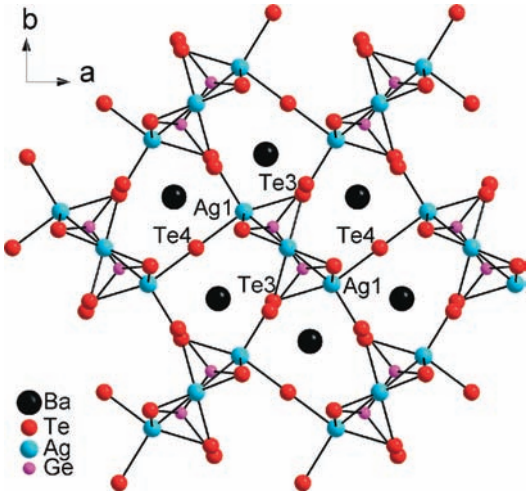

Figure 4. A larger view of the covalent framework of $Ba_4Ag_{3.95}Ge_2Te_9$ encompassing the Ba atoms.

at the bottom of the valence band, while the Cu d states mostly occur between −2 and −4 eV (Figure 5). The model calculation with the Cu_3 cluster, formula $Ba_4Cu_3Ge_2Te_9$, indicates a much smaller gap of 0.3 eV, and the Fermi level is located 0.2 eV below the gap, indicative of a *p*-doped semiconductor. The model of $Ba_4Cu_3Ge_2Te_9$ is less important for the properties, however, because it is based on the Cu2A atom with its 12% occupancy.

To gain insight into the character of the two metal−metal contacts per cluster, the crystal orbital Hamilton population curves[49,50] of both compounds are compared in Figure 6. The major contributions come from the respective d orbitals and are thus mostly well below the Fermi level. Therefore, small decreases of the valence-electron numbers caused by the Ag/Cu deficiencies will have only a minor impact on the strength of these interactions. The integration up to the Fermi-level reveals that all five shown interactions have net bonding character, reflected in negative integrated crystal orbital Hamilton populations (ICOHPs).[51] For the Ag compound, these are −0.39 eV (2.89 Å) and −0.33 eV (3.04 Å), and for the Cu compound, they are −0.82 eV (2.46 Å) and −0.42 eV (2.76 Å). That is, in each case, the shorter bond is the stronger one. In the $Ba_4Cu_3Ge_2Te_9$ model, only one (longer) Cu−Cu contact of 2.83 Å exists with a smaller ICOHP of −0.23 eV. Again, slight decreases of the valence electron concentration caused by the Ag/Cu deficiencies can only have a minor impact on the bond strengths, because the states directly below the Fermi level are basically nonbonding.

Physical Properties. The property measurements verified the semiconducting character. Almost exponential increases of the electrical conductivity with increasing temperature were observed for both tellurides (left part of Figure 7), which is typical for semiconductors. That the temperature dependence is not exactly exponential reaffirms the observation that the materials exhibit

(46) Mehrotra, P. K.; Hoffmann, R. *Inorg. Chem.* **1978**, *17*, 2187–2189.
(47) Merz, K. M.Jr.; Hoffmann, R. *Inorg. Chem.* **1988**, *27*, 2120–2127.
(48) Pyykkö, P. *Chem. Rev.* **1997**, *97*, 597–636.
(49) Dronskowski, R.; Blöchl, P. E. *J. Phys. Chem.* **1993**, *97*, 8617–8624.
(50) Glassey, W. V.; Hoffmann, R. *J. Chem. Phys.* **2000**, *113*, 1698–1704.
(51) Landrum, G. A.; Dronskowski, R. *Angew. Chem., Int. Ed.* **2000**, *39*, 1560–1585.

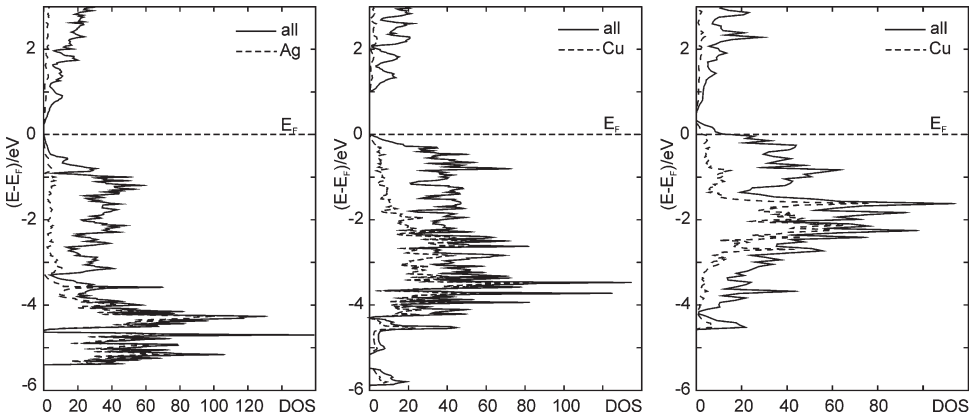

Figure 5. Densities of states of $Ba_4Ag_4Ge_2Te_9$ (left), $Ba_4Cu_4Ge_2Te_9$ (center), and $Ba_4Cu_3Ge_2Te_9$ (right).

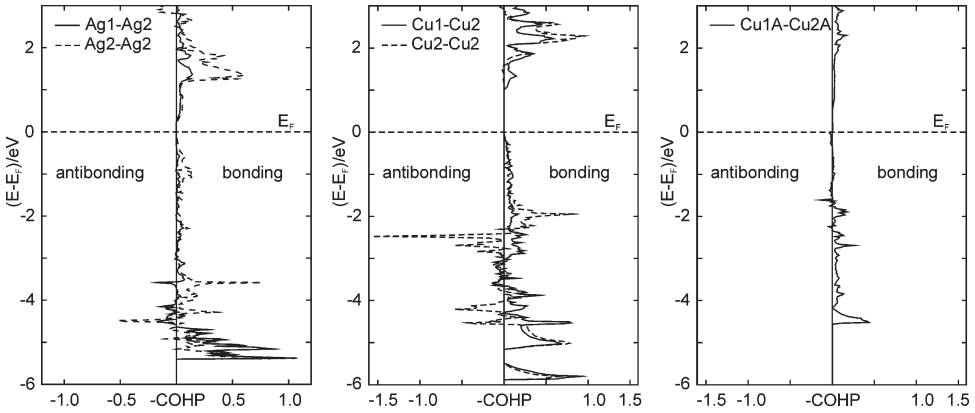

Figure 6. Metal−metal crystal orbital Hamilton population curves of $Ba_4Ag_4Ge_2Te_9$ (left), $Ba_4Cu_4Ge_2Te_9$ (center), and $Ba_4Cu_3Ge_2Te_9$ (right).

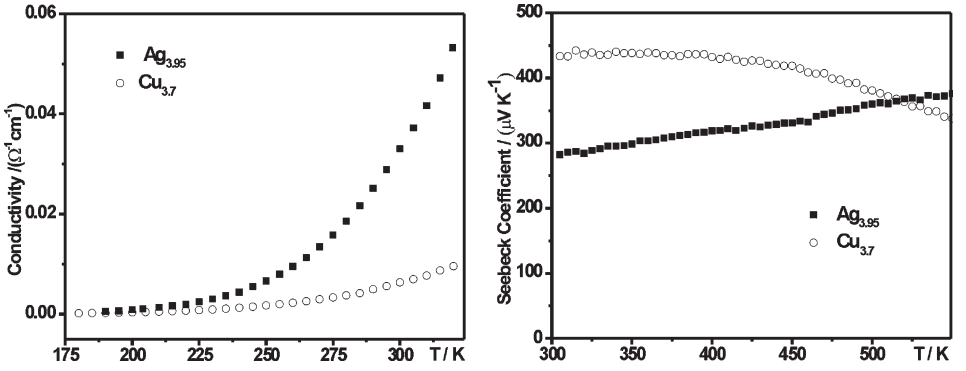

Figure 7. Electrical conductivity (left) and Seebeck coefficient (right) of $Ba_4Ag_{3.95}Ge_2Te_9$ and $Ba_4Cu_{3.7}Ge_2Te_9$.

Ag/Cu deficiencies and thus extrinsic charge carriers (namely, holes) in addition to the thermally activated carriers. The electrical conductivity is higher in the case of the silver compound, which is consistent with the smaller calculated band gap of $Ba_4Ag_4Ge_2Te_9$, compared to $Ba_4Cu_4Ge_2Te_9$.

The positive values of the Seebeck coefficient reveal that *p*-type carriers are dominant in both compounds. For $Ba_4Ag_{3.95}Ge_2Te_9$, the Seebeck coefficient increases with increasing temperature from 282 μV/K to 376 μV/K between 305 and 550 K (right part of Figure 7). For $Ba_4Cu_{3.71}Ge_2Te_9$, the Seebeck coefficient is relatively constant at 430−440 μV/K between 305 and 340 K, and then it decreases with increasing temperature down to 338 μV/K at 550 K. On the basis of the equation $E_g = 2 \cdot e \cdot S_{max} \cdot T_{max}$,[52] the band gap, E_g, is estimated to be between 0.26 and 0.32 eV.

Conclusions

We have successfully synthesized and characterized two new tellurides, $Ba_4Ag_{3.95}Ge_2Te_9$ and $Ba_4Cu_{3.71}Ge_2Te_9$, that contain low-valent Ge. Ignoring the split sites in the case of the Cu compounds, these materials form the same new structure type, containing both Ag−Ag/Cu−Cu and Ge−Ge bonds. Both materials exhibit only a small phase width, as analyzed via different single-crystal structure studies. The various split sites of the Cu compound give rise to different Cu−Te coordination polyhedra and Cu clusters, for example, a linear Cu_3 unit in addition to the planar Cu_4 cluster.

(52) Goldsmid, H. J.; Sharp, J. W. *J. Electron. Mater.* **1999**, *28*, 869–872.

Both materials are hole-doped semiconductors, with calculated gaps of 0.24 and 1.0 eV. The electrical conductivity is too low for thermoelectric materials, despite the hole doping that originates from the Ag/Cu deficiencies.

Acknowledgment. Financial support from NSERC, CFI, OIT (Ontario Distinguished Researcher Award for H.K.), the Province of Ontario (Premier's Research Excellence Award for H.K.), and the Canada Research Chair program (CRC for H.K.) is appreciated.

Supporting Information Available: One crystallographic information file (CIF). This material is available free of charge via the Internet at http://pubs.acs.org.